ACS Sustainable Chemistry & Engineering

Research Article

pubs.acs.org/journal/ascecg

Preparation of Flexible, Highly Transparent, Cross-Linked Cellulose Thin Film with High Mechanical Strength and Low Coefficient of Thermal Expansion

Bingqian Guo, Wufeng Chen, and Lifeng Yan*

Hefei National Laboratory for Physical Sciences at the Microscale and Department of Chemical Physics, CAS Key Laboratory of Soft Matter Chemistry, University of Science and Technology of China, Hefei 230026, P.R. China

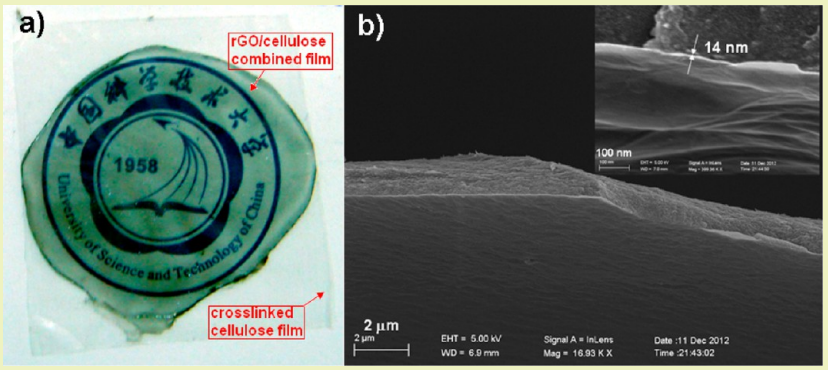

ABSTRACT: The development of next generation of flexible electronic devices requires new materials to replace the glass as transparent windows. Here, flexible, transparent, and very strong cross-linked celluloses have been prepared by cross-linking free cellulose chains with epichlorohydrin (ECH) in its aqueous solution. Atomic force microscopy (AFM), light transmittance, differential thermogravimetric (DTG) thermal analyses, and tensile tests revealed that the as-prepared films are a thickness of about 10 μm with highly optical transparency and mechanical strength. The film also showed a low coefficient of thermal expansion (CTE) of about 6.9 ppm/K, which is superior to that of glass. Then the as-prepared cellulose film was combined with a dried foam ultrathin film of reduced graphene oxide to prepare a new, flexible, transparent, very strong, and electrically conductive thin film.

KEYWORDS: *Cellulose, Cross-linked, Thin film, Transparent, High strength*

INTRODUCTION

Optically transparent substrates such as glass are widely utilized in the flat-panel display (FPD) devices.[1] However, glass is fragile, and it is difficult to prepare large or foldable display. Polymeric materials have been paid much attention for possibly replacing glass because of their processing and foldable properties.[2,3] However, most of the reported polymers have large coefficients of thermal expansion (CTE) of about 50−200 ppm/K, while it is only about 9 ppm/K for glass.[4] There is usually thermal damage of functional materials deposited on them during fabrication or application. Therefore, it is still a challenging and attractive topic to develop new polymeric composites with both optical transparency and low CTE.[5]

Recently, cellulose-based optically transparent materials have been developed.[4,6−11]As the major component of plant biomass, cellulose usually forms nanofibers with diameters of 15−20 nm with a complex hydrogen bonding system. It is well known that cellulose nanofibers have a CTE of 0.1 ppm/K and an estimated strength of 2−3 GPa.[12,13] Cellulose nanofibers are virtually free from light scattering, which makes it possible to prepare optically transparent films or papers.[14] Bacterial cellulose (BC) is the major resource of cellulose that has been widely used to prepare optically transparent composites after different modifications.[6−8,15] However, cellulose nanofibers were used directly in all of the studies, and their crystalline structures were reserved in the final products, which make the products anisotropic at the microscale and maybe harmful for refined display. In addition, it is difficult to prepare very thin films of cellulose nanofibers in the size of micrometers, and the decrease in the thickness of the film is helpful to develop ingenious devices.[2] Among the reported methods, hot-press and polishing are usually required to make the film compact and more optically transparent, and special devices are required as reported.[4]

Recently, some reports have been published on the preparation of cellulose-based films in the thickness of millimeters by regeneration or blending with other polymers for better mechanical properties.[16−18] However, less attention had been paid to the preparation of isotropic thin films of

Received: July 25, 2013
Revised: August 27, 2013
Published: August 28, 2013

cellulose in the thickness of micrometers with highly optical transparency, high mechanical properties, and low CTE.

Here, we developed a method to prepare isotropic cellulose thin film with a thickness of about 10 μm with highly optical transparency, high mechanical properties, hydrophobicity, and low CTE by cross-linking of the dissolved cellulose with epichlorohydrin (ECH) in its aqueous solution. The mixture of aqueous solution of sodium hydroxide and urea was chosen as the solvent for cellulose in this study.[16] Then, the as-prepared cellulose film was covered by the ultrathin film of graphene oxide, and after reduction, it should result in a combined graphene/cellulose thin film, which has the potential to be used as a transparent and electrically conductive film.

EXPERIMENTAL SECTION

Materials. Microcrystalline cellulose powder (M_w = 1.08 × 10^5 g/mol by an Ubbelohde viscometer using DMAc/LiCl as solvent) was purchased from Shanghai Hengxin Chemical Reagent Co. Ltd. Sodium hydroxide, urea, and epichlorohydrin were all analytical grade, and trimethylamine was used as a 33% aqueous solution; all purchased from Sinopharm Chemical Reagent Co. Ltd. Deionized water with a resistivity of 18 MΩ cm was produced by Milli-Q (Millipore, U.S.A.) and was used for solution preparation. Graphite powder (natural briquetting grade, about 100 mesh, 99.9995% (metals basis)) was purchased from Alfa Aesar. Analytical grade Vitamin C, $KMnO_4$, 98% H_2SO_4, 30% H_2O_2 aqueous solution, and acrylic acid were purchased from Shanghai Chemical Reagents Company and were used directly without further purification.

Preparation of Cross-Linked Cellulose Thin Film in Aqueous Solution. A total of 4.5 g of NaOH, 3.0 g of urea, and 67.5 g of deionized water were added into a flask, and a mixture was obtained under stirring. Then, the mixture was pre-cooled at 4 °C for 2h, and 2.25−3.75 g of microcrystalline cellulose was added under stirring. The as-formed suspension was cooled at −20 °C for 12 h, and then it was thawed under strong stir at room temperature. At the end, the homogeneous cellulose solutions with concentration of 3−5 wt % were obtained.[16] Next, 0.4−1.6 mL epichlorohydrin (ECH) was added into the 25 mL cellulose solutions under stirring to obtain a homogeneous solution, and then the solution was put into a Petri dish to form a liquid layer at the bottom. After it was heated at 80 °C for 3 h, a solid film was formed. The film was then washed with 5% acetic acid aqueous solution and deionized water and was dried at 40 °C in an oven. A control cellulose film without cross-linking was also prepared by a similar process. Table 1 is a summary the preparation of the thin films.

Table 1. Preparation of Cross-Linked and Regenerated Cellulose Thin Films

samples	A	B	C	regenerated cellulose film
concentration of cellulose solution (wt %)	3.0	4.0	5.0	5.0
cross-linker ECH[a] (mL)	1.6	0.7	0.4	0

[a]In 25 mL of cellulose solution.

Preparation of Graphene Oxide (GO). GO is prepared from natural graphite by the well-known Hummers and Offema method.[19] The obtained powder was redispersed into water and was treated by mild ultrasound for 15 min. A homogeneous suspension is collected after filtering the trace black residues. GO powder was obtained after freezing and drying of the suspension.

Preparation of Centimeter-Sized Ultrathin Dried Foam Film of GO. The preparation of centimeter-sized ultrathin dried foam film of GO was carried out according to our recently reported method.[20] In brief, aqueous solutions of GO in different concentrations (4.0 mg/mL) were first prepared by dispersing GO in deionized water under mild ultrasound for 15 min, and then a small quantity of surfactant, such as CTAB (0.02 mg/mL), was added. Then a ring of Ag wire was vertically dipped into the solution and gently lifted out. A small volume of aqueous solution of GO was captured by the template during the process, and the liquid film was then allowed to dry in air.

Combination of Cellulose and GO Films and the Reduction for Cellulose/Reduced Graphene Oxide (rGO) Film. A circular dried GO ultrathin film was transferred onto the surface of an as-prepared cross-linked cellulose film blown by nitrogen gas, and then it was reduced by a concentrated ethanol solution of HI (30 v %) for 6 h at room temperature followed by an ethanol wash; the process was repeated twice in order to increase the reducing degree.

Characterization. Light transparencies of the films were measured using an SP-721E UV−vis spectrophotometer (Shanghai Spectrum Instruments Co. Ltd., China). DTG curves were obtained by a Shimadzu TGA-50 thermogravimetric instrument, and the temperature range employed is 30−700 °C with a heating rate of 10 °C/min. The surface structures of the composites were measured using atomic force microscopy (AFM, Nanoscope III A, DI). AFM images were captured in the contact mode by a Si_3N_4 tip (DI). The scan rates were in between 1.0 and 2.4 Hz. The tensile strength (σ_B) and elongation at break (ε_B) of the composites were measured on a universal tensile tester (TS7104, Shenzhen SANS Test machine, China) according to ISO527-3:1995 at a speed of 5.0 mm/min. The specimens were in a rectangular shape with a dimension of 10 mm × 40 mm. The length between two grips was set as 10 mm. Each testing was repeated on five specimens, and the mean values as well as standard deviations were reported. The CTEs of the cellulose films were measured using a thermomechanical analyzer (TMA-SS6100, Seiko Instruments). For the electrical conductivity measurement, the combined cellulose/rGO film was patterned with 100 nm gold contacts through a shadow mask, and then the sheet resistance was measured using a semiconductor parametric analyzer (Keithley 2420, Keithley Instruments Inc., Cleveland, OH).[21]

RESULTS AND DISCUSSION

Figure 1 shows the photographs of the as-prepared cellulose thin films using different concentrations of cellulose aqueous solution and cross-linker. Cross-linking degrees were controlled by the content of the cross-linker ECH (Table 1). Clearly, all three samples show highly optical transparency, and the words on the paper behind the film can be distinguished clearly. AFM measurements showed that the as-prepared cross-linked cellulose films are flat, with roughness (RMS) of 4.70, 3.75, and 7.25 nm, indicating the homogemeous dispersant of cellulose chains in the cross-linked network. In addition, it seems that there exists an optimal ratio of ECH to cellulose for an homogeneous cross-linking. As a control, a no cross-linked cellulose film was prepared by regenerating the cellulose in a acidic aqueous solution. Figure 2 show its typical AFM images in both height and phase signals. Clearly, the film is more coarse than that of the cross-linked film, indicating the recrystallization of cellulose chains is not homogeneous in large range.

Figure 3 shows the light transparences of the three films. The values of all the films reaches up to 84.4%, and it is up 90.7% for Sample C. The microstructures of the films measured by AFM (Figure 1c,d) also showed that all the films are dense, and no typical cellulose nanofibers could be observed. It reveals that cellulose has been well dissolved and cross-linked, which results in the highly optical transparency. The result also reveals that the low concentration of cellulose solution favors the high light transparency.

TGA and DGA curves of the cross-linked cellulose thin film (Sample B) were shown in Figure 4. As a control, both the TGA and DHA curves of the regenerated cellulose film prepared by 5 wt % cellulose solution without cross-linker are

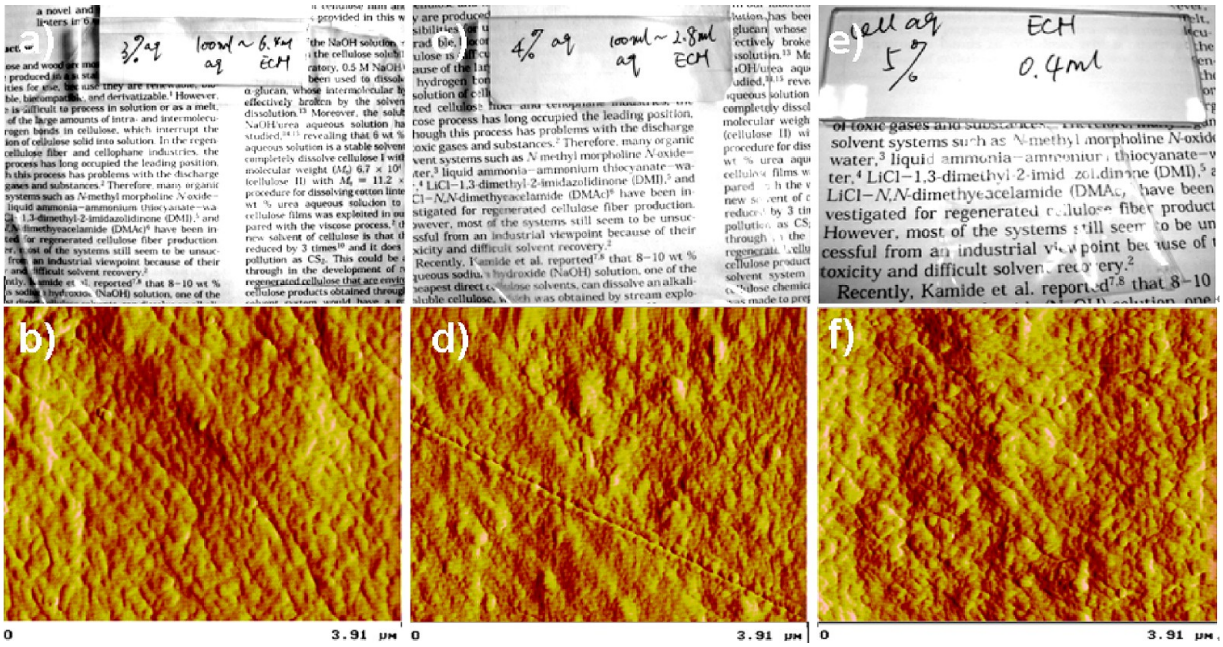

Figure 1. Photographs and AFM images of the cellulose cross-linked thin films prepared by different concentrations of cellulose aqueous solution and cross-linker ECH. Sample A (a,b) cellulose: 3.0 wt %, ECH: 6.4 v/v %. Sample B (c, d) cellulose: 4.0 wt %, ECH: 2.8 v/v %. Sample C (e,f) cellulose: 5.0 wt %, ECH: 1.6 v/v %.

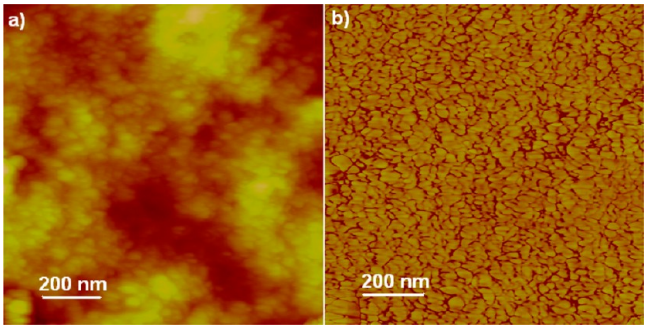

Figure 2. Typical AFM height (a) and phase (b) images of no cross-linked regenerated cellulose film.

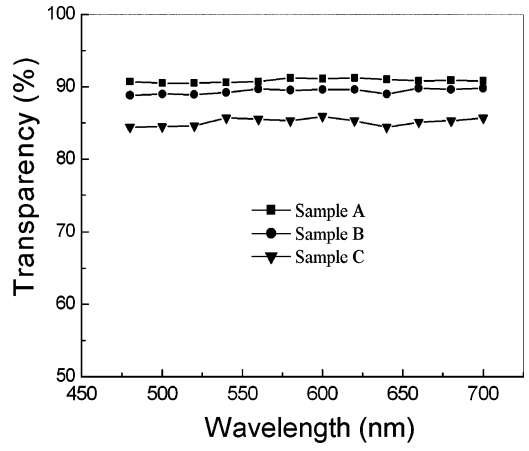

Figure 3. Light transparency of the cross-linked cellulose thin films.

also shown. The results reveal that the thermal stability of the film increases after cross-linking. The decomposition temperature of the cross-linked film is about 345 °C, while it is 304 °C for the regenerated cellulose film, and the cross-linked cellulose thin film is much thermal-stable than that of the regenerated film. The result is positive for its potential application in electronic devices.

Figure 5 shows the X-ray diffraction profiles of the cellulose, regenerated cellulose, and cross-linked cellulose thin films. For cellulose, the pattern exhibits the typical diffraction peaks at 14.8°, 16.2°, 22.7°, and 34.3°, which belong to the crystalline structure of cellulose I.[16] For the regenerated cellulose film, the XRD pattern demonstrates the two typical diffractions at 2θ = 19.7° and 21.9°, which correspond to the crystalline structure of cellulose II.[16] However, for the cross-linked cellulose thin film (sample A and B), the intensity of the diffractions are very weak, indicating damage of the crystalline structure of cellulose during the dissolving and cross-linking process. But for sample C, which was prepared with the 5 wt % aqueous solution of cellulose with 1.6% ECH, the typical diffractions for the crystalline structure of cellulose II appears again, indicating part of the cellulose was not cross-linked; they were regenerated during the film formation.

Figure 6 shows the FT-IR spectra of regenerated cellulose film and cross-linked cellulose films. In comparison to pure cellulose, the peaks at about 1230 cm^{-1} could be attributed to the vibration of the C−N bond in the cross-linking network, and the new peak appearing at 2880 cm^{-1} corresponds to the CH_2N vibration.[22] Clearly, the more cross-linker that was used, the stronger the signal appeared, indicating a high degree of cross-linking. The degree of cross-linking of sample A is much higher than that of the other two samples.

Figure 7 shows the typical stress−strain (σ vs ε) curves for the regenerated and cross-linked cellulose thin films. Compared with the regenerated cellulose thin film, the tensile strengths at break of the cross-linked cellulose thin films (samples B and C) increase hugely, indicating that cross-linking can effectively change the mechanical strength of the thin film, and the σ_{max} values increased sharply from 50.6 to 336.1 MPa (sample B) and 375.6 MPa (sample C). The elongation at break (ε_B) also

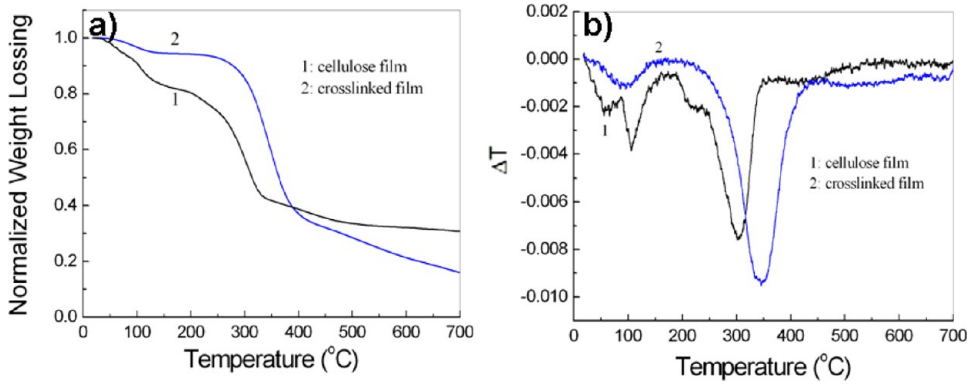

Figure 4. (a) TGA and (b) DGA curves of the regenerated and cross-linked (sample B) cellulose thin films.

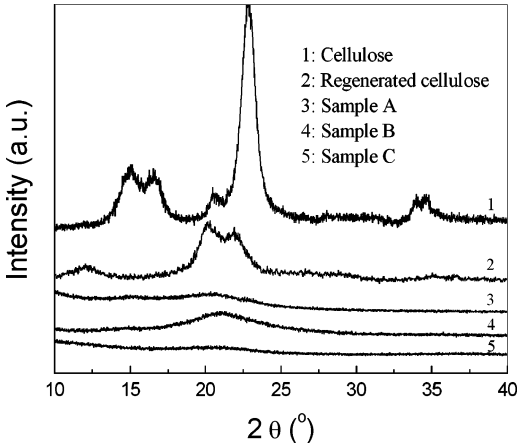

Figure 5. X-ray diffraction profiles of the cellulose, regenerated cellulose, and cross-linked cellulose thin films (samples A, B, and C).

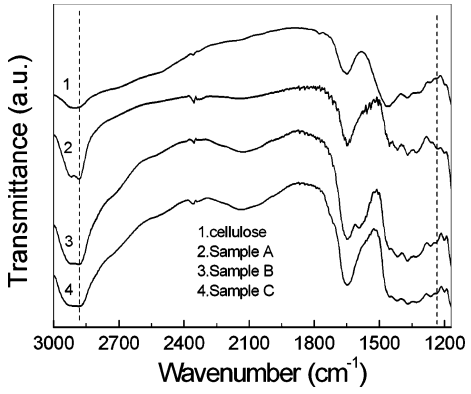

Figure 6. FT-IR spectra of cellulose and cross-linked cellulose thin films (samples A, B, C).

changes slight from 7.14% to 11.55% (sample B) and 15.97% (sample C). However, for sample A, the tensile strength at break is smaller than that of the regenerated cellulose thin film, while it shows a high elongation at break of 89.8%, indicating that the cross-linked cellulose thin film prepared by the low concentration of cellulose solution (3 wt %) makes the film more soft though it has a high degree of cross-linking. The Young's modulus of the regenerated and cross-linked cellulose thin films are also shown as an inset in Figure 7. For the cross-linked cellulose thin films, the Young's modulus values are 0.45, 4.9, and 6.6 GPa for sample A, sample B, and sample C, respectively, while it is 0.77 GPa for the regenerated cellulose thin film.

The cross-linking of cellulose should make the cellulose chains interact with each other through the cross-linker to form a network and restrict the thermal expansion of the cellulose chains. It has been reported that the CTE of the cellulose matrix regenerated from its LiCl/DMAc solution is about 14 ppm/K.[13] Here, the CTE of sample B is about 6.9 ppm/K, and the value is superior to that of glass and other reported polymers. So, it is possible to use the as-prepared film instead of glass as an optically transparent layer for OLEDs. The as-prepared film is isotropic. Figure 8 shows its polarized optical microscopy (POM) image, and no typical texture of the cellulose crystalline appears, indicating the homogeneous distribution of cellulose molecules inside the film. However, the anisotropic phase can be found after the film was elongated and broken at the edge (Figure 8b), indicating that the cellulose chains could be rearranged and form the cellulose alignment driven by external force. The cross-linked cellulose thin film becomes much hydrophobic than that of the regenerated cellulose thin film, and the contact angles for sample A, sample B, sample C, and the regenerated cellulose thin film are 91.3°, 75.5°, 74.4°, and 17.3°, respectively.

Indium tin oxide (ITO) and fluorine tin oxide (FTO) have been widely applied in optoelectronic devices due to their high electrical conductivity and transparency. However, some disadvantages appear, such as the (i) increasing cost and limited storage of indium on earth, (ii) complicated processing, (iii) sensitivity to acid and basic environments, (iv) brittle nature, which limits its application in flexible devices, and (v) limited transparency in the near-infrared region. Recently, many efforts have been made to search for new electrode materials to replace of ITO and FTO with good stability, high electrical conductivity, and transparency. For example, metal grids,[23] metallic nanowires,[24] and carbon nanotubes (CNT)[25] have been developed. Recently, Cui et al. reported the preparation of conductive cellulose film by coating conducting materials (CNT or ITO) onto the surface of nanocellulose paper.[26] However, it is still necessary to find novel materials for the target.

Graphene is a potential material to replace indium tin oxide (ITO) or fluorine tin oxide (FTO) due to its remarkabe electronic properties for transparent electrode materials.[27] It has been reported that the transparency of mechanically exfoliated graphene is 97.7%, and for graphene synthesized by chemical vapor deposition, (CVD) it is 97.4%.[28,29] New methods had been developed for the preparation of graphene

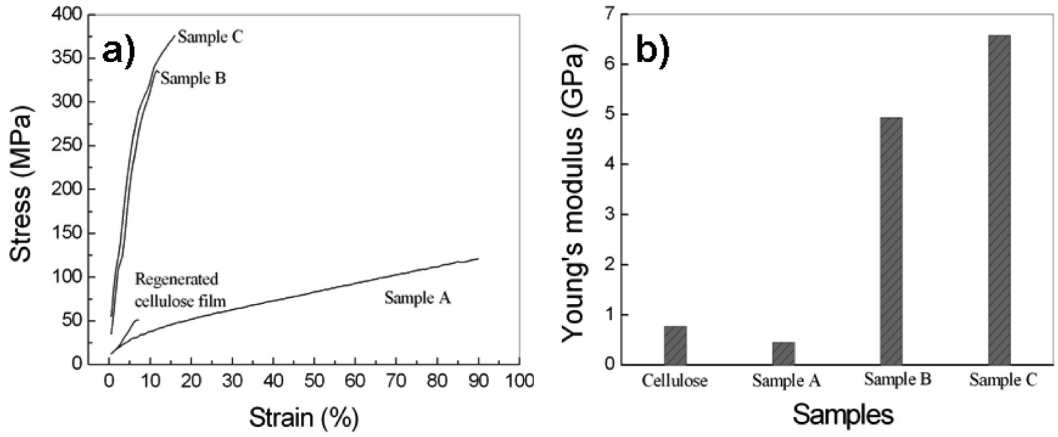

Figure 7. (a) Stress–strain curve of the regenerated and cross-linked cellulose thin films (samples A, B, C) and the Young's modulus of the thin films (b).

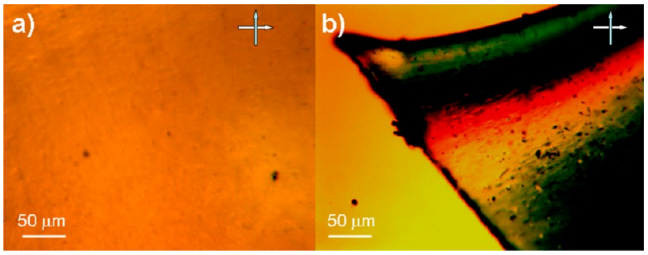

Figure 8. POM images of cross-linked cellulose film (sample C) before (a) and after it was stretched and broken (edge).

film with high electrical conductivity and transparency, especially at a large scale, such as Langmuir–Blodgett (LB),[30] vacuum filtration,[31] evaporation-induced self-assembly,[32] spray coating,[33] spin coating,[21] and bubble deposition[34] methods. Recently, we reported a novel and simple method to fabricate centimeter-sized dried foam thin films of reduced graphene oxide via drying the relative foam liquid film supported by a rigid frame following a reduction.[20] The maximum transparency is 75.8%, while the minimum sheet resistance R_s is 920 Ω/m, indicating that they are the potential materials to replace ITO or FTO in optoelectrical devices. For flexible devices, the combination of the rGO ultrathin film with a transparent polymer support is required, especially for low CTE polymers.

As our previous report, dried foam film of GO can be easily prepared.[20] The as-formed GO ultrathin films can be transferred to different kinds of substrates, such as flexible polymers. Here, a circular dried GO ultrathin film was transferred onto the surface of a cross-linked cellulose film, and then it was reduced by concentrated HI ethanol solution. Figure 9a shows the macroscopic image of the sample, which remains highly transparent (65%), and it makes a potential ultrathin film for flexible electronics. The electrical conductivities of the flexible combined cellulose/rGO thin films were measured by a two-point-probe method and the R_s is 980 Ω/m, and it still remains to be 1.02 kΩ/m after repeated bending for 100 times, indicating that the bending process exhibits less effect on its microstructure. Figure 9b shows the SEM sectional image of the combined thin film, and both the cellulose and rGO films are incorporated closely. The thickness of the covered rGO layer is about 14 nm.

CONCLUSIONS

In summary, a new method was reported to prepare cross-linked cellulose thin films with highly optical transparency, high mechanical strength, hydrophobicity, isotropy, and low CTE. After it was combined with a dried foam ultrathin film of graphene oxide following a chemical reduction, a flexible, transparent, very strong, and electrically conductive cellulose/rGO thin film was prepared. The as-prepared film is a potential material for the next generations of electronic devices.

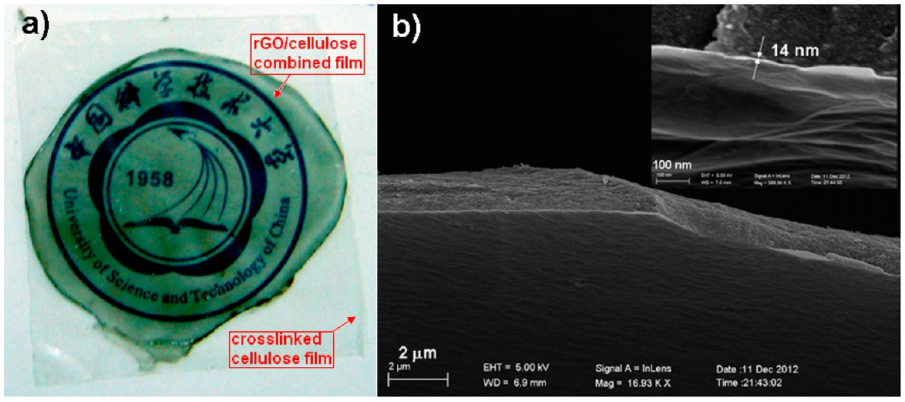

Figure 9. Photograph (a) and SEM (b) images of the as-formed cross-linked cellulose/rGO combined thin film. Inset shows the thickness of the covered rGO ultrathin film.

AUTHOR INFORMATION

Corresponding Author

*E-mail: lfyan@ustc.edu.cn. Fax: +86-551-3603748. Tel: +86-551-63606853.

Notes

The authors declare no competing financial interest.

ACKNOWLEDGMENTS

This work is supported by the National High Technology Research and Development Program (No. 2012AA051803) and the National Basic Research Program of China (No. 2011CB921403 and 2010CB923302).

REFERENCES

(1) Lipomi, D. J.; Bao, Z. Stretchable, elastic materials and devices for solar energy conversion. *Energy Environ. Sci.* **2011**, *4* (9), 3314−3328.
(2) Forrest, S. R. The path to ubiquitous and low-cost organic electronic appliances on plastic. *Nature* **2004**, *428* (6986), 911−918.
(3) Yuan, L.; Yao, B.; Hu, B.; Huo, K.; Chen, W.; Zhou, J. Polypyrrole-coated paper for flexible solid-state energy storage. *Energy Environ. Sci.* **2013**, *6* (2), 470−476.
(4) Nogi, M.; Yano, H. Optically transparent nanofiber sheets by deposition of transparent materials: A concept for a roll-to-roll processing. *Appl. Phys. Lett.* **2009**, *94*, 23.
(5) Kim, D. H.; Rogers, J. A. Stretchable electronics: Materials strategies and devices. *Adv. Mater.* **2008**, *20* (24), 4887−4892.
(6) Nogi, M.; Yano, H. Transparent nanocomposites based on cellulose produced by bacteria offer potential innovation in the electronics device industry. *Adv. Mater.* **2008**, *20* (10), 1849−1852.
(7) Nogi, M.; Ifuku, S.; Abe, K.; Handa, K.; Nakagaito, A. N.; Yano, H. Fiber-content dependency of the optical transparency and thermal expansion of bacterial nanofiber reinforced composites. *Appl. Phys. Lett.* **2006**, *88*, 133124.
(8) Nogi, M.; Handa, K.; Nakagaito, A. N.; Yano, H. Optically transparent bionanofiber composites with low sensitivity to refractive index of the polymer matrix. *Appl. Phys. Lett.* **2005**, *87*, 243110.
(9) Nogi, M.; Abe, K.; Handa, K.; Nakatsubo, F.; Ifuku, S.; Yano, H. Property enhancement of optically transparent bionanofiber composites by acetylation. *Appl. Phys. Lett.* **2006**, *89*, 233123.
(10) Iwamoto, S.; Nakagaito, A. N.; Yano, H.; Nogi, M. Optically transparent composites reinforced with plant fiber-based nanofibers. *Appl. Phys. A: Mater. Sci. Process.* **2005**, *81* (6), CP8−1112.
(11) Zhao, Y.; Chen, W. F.; Yuan, C. F.; Zhu, Z. Y.; Yan, L. F. Hydrogenated graphene as metal-free catalyst for Fenton-like reaction. *Chin. J. Chem. Phys.* **2012**, *25* (3), 335−338.
(12) Shimazaki, Y.; Miyazaki, Y.; Takezawa, Y.; Nogi, M.; Abe, K.; Ifuku, S.; Yano, H. Excellent thermal conductivity of transparent cellulose nanofiber/epoxy resin nanocomposites. *Biomacromolecules* **2007**, *8* (9), 2976−2978.
(13) Nishino, T.; Matsuda, I.; Hirao, K. All-cellulose composite. *Macromolecules* **2004**, *37* (20), 7683−7687.
(14) Yano, H.; Sugiyama, J.; Nakagaito, A. N.; Nogi, M.; Matsuura, T.; Hikita, M.; Handa, K. Optically transparent composites reinforced with networks of bacterial nanofibers. *Adv. Mater.* **2005**, *17* (2), 153−155.
(15) Ifuku, S.; Nogi, M.; Abe, K.; Handa, K.; Nakatsubo, F.; Yano, H. Surface modification of bacterial cellulose nanofibers for property enhancement of optically transparent composites: Dependence on acetyl-group DS. *Biomacromolecules* **2007**, *8* (6), 1973−1978.
(16) Zhang, L.; Mao, Y.; Zhou, J. P.; Cai, J. Effects of coagulation conditions on the properties of regenerated cellulose films prepared in NaOH/urea aqueous solution. *Ind. Eng. Chem. Res.* **2005**, *44* (3), 522−529.
(17) Yang, Q. L.; Lue, A.; Qi, H. S.; Sun, Y. X.; Zhang, X. Z.; Zhang, L. N. Properties and bioapplications of blended cellulose and corn protein films. *Macromol. Biosci.* **2009**, *9* (9), 849−856.
(18) Liu, S. L.; Zhang, L. N.; Sun, Y. X.; Lin, Y.; Zhang, X. Z.; Nishiyama, Y. Supramolecular structure and properties of high strength regenerated cellulose films. *Macro. Biosci* **2009**, *9* (1), 29−35.
(19) Chen, W. F.; Yan, L. F.; Bangal, P. R. Preparation of graphene by the rapid and mild thermal reduction of graphene oxide induced by microwaves. *Carbon* **2010**, *48* (4), 1146−1152.
(20) Chen, W.; Yan, L. Centimeter-sized dried foam films of graphene: Preparation, mechanical and electronic properties. *Adv. Mater.* **2012**, *24* (46), 6229−6233.
(21) Becerril, H. A.; Mao, J.; Liu, Z.; Stoltenberg, R. M.; Bao, Z.; Chen, Y. Evaluation of solution-processed reduced graphene oxide films as transparent conductors. *ACS Nano* **2008**, *2* (3), 463−470.
(22) Yan, L. F.; Shuai, Q.; Gong, X. L.; Gu, Q.; Yu, H. Q. Synthesis of microporous cationic hydrogel of hydroxypropyl cellulose (HPC) and its application on anionic dye removal. *Clean: Soil, Air, Water* **2009**, *37* (4−5), 392−398.
(23) De, S.; Higgins, T. M.; Lyons, P. E.; Doherty, E. M.; Nirmalraj, P. N.; Blau, W. J.; Boland, J. J.; Coleman, J. N. Silver nanowire networks as flexible, transparent, conducting films: Extremely high DC to optical conductivity ratios. *Acs Nano* **2009**, *3* (7), 1767−1774.
(24) Lee, J. Y.; Connor, S. T.; Cui, Y.; Peumans, P. Solution-processed metal nanowire mesh transparent electrodes. *Nano Lett.* **2008**, *8* (2), 689−692.
(25) Wu, Z. C.; Chen, Z. H.; Du, X.; Logan, J. M.; Sippel, J.; Nikolou, M.; Kamaras, K.; Reynolds, J. R.; Tanner, D. B.; Hebard, A. F.; Rinzler, A. G. Transparent, conductive carbon nanotube films. *Science* **2004**, *305* (5688), 1273−1276.
(26) Hu, L.; Zheng, G.; Yao, J.; Liu, N.; Weil, B.; Eskilsson, M.; Karabulut, E.; Ruan, Z.; Fan, S.; Bloking, J. T.; McGehee, M. D.; Wagberg, L.; Cui, Y. Transparent and conductive paper from nanocellulose fibers. *Energy Environ. Sci.* **2013**, *6* (2), 513−518.
(27) Gwon, H.; Kim, H.-S.; Lee, K. U.; Seo, D.-H.; Park, Y. C.; Lee, Y.-S.; Ahn, B. T.; Kang, K. Flexible energy storage devices based on graphene paper. *Energy Environ. Sci.* **2011**, *4* (4), 1277−1283.
(28) Kim, K. S.; Zhao, Y.; Jang, H.; Lee, S. Y.; Kim, J. M.; Ahn, J. H.; Kim, P.; Choi, J. Y.; Hong, B. H. Large-scale pattern growth of graphene films for stretchable transparent electrodes. *Nature* **2009**, *457* (7230), 706−710.
(29) Li, X. S.; Cai, W. W.; An, J. H.; Kim, S.; Nah, J.; Yang, D. X.; Piner, R.; Velamakanni, A.; Jung, I.; Tutuc, E.; Banerjee, S. K.; Colombo, L.; Ruoff, R. S. Large-area synthesis of high-quality and uniform graphene films on copper foils. *Science* **2009**, *324* (5932), 1312−1314.
(30) Li, X.; Zhang, G.; Bai, X.; Sun, X.; Wang, X.; Wang, E.; Dai, H. Highly conducting graphene sheets and Langmuir−Blodgett films. *Nat Nano* **2008**, *3* (9), 538−542.
(31) De, S.; King, P. J.; Lotya, M.; O'Neill, A.; Doherty, E. M.; Hernandez, Y.; Duesberg, G. S.; Coleman, J. N. Flexible, transparent, conducting films of randomly stacked graphene from surfactant-stabilized, oxide-free graphene dispersions. *Small* **2010**, *6* (3), 458−464.
(32) Chen, C.; Yang, Q.-H.; Yang, Y.; Lv, W.; Wen, Y.; Hou, P.-X.; Wang, M.; Cheng, H.-M. Self-assembled free-standing graphite oxide membrane. *Adv. Mater.* **2009**, *21* (29), 3007 +..
(33) Blake, P.; Brimicombe, P. D.; Nair, R. R.; Booth, T. J.; Jiang, D.; Schedin, F.; Ponomarenko, L. A.; Morozov, S. V.; Gleeson, H. F.; Hill, E. W.; Geim, A. K.; Novoselov, K. S. Graphene-based liquid crystal device. *Nano Lett.* **2008**, *8* (6), 1704−1708.
(34) Azevedo, J. l.; Costa-Coquelard, C.; Jegou, P.; Yu, T.; Benattar, J.-J. Highly ordered monolayer, multilayer, and hybrid films of graphene oxide obtained by the bubble deposition method. *J. Phys. Chem. C* **2011**, *115* (30), 14678−14681.